Anthropogenic and meteorological influences on PM$_{10}$ metal/semi-metal concentrations: Implications for human health

Luis Negral [a, *], Beatriz Suárez-Peña [b], Eugenia Zapico [a], Yolanda Fernández-Nava [a], Laura Megido [a], Jose Moreno [c], Elena Marañón [a], Leonor Castrillón [a]

[a] Department of Chemical and Environmental Engineering, Polytechnic School of Engineering, Gijón Campus, University of Oviedo, 33203, Gijón, Spain
[b] Department of Materials Science and Metallurgical Engineering, Polytechnic School of Engineering, Gijón Campus, University of Oviedo, 33203, Gijón, Spain
[c] Department of Chemical and Environmental Engineering, Technical University of Cartagena, 30202, Cartagena, Spain

A B S T R A C T

There is growing interest in investigating the human health risk associated with metals in airborne particulate matter. The objective of this paper is the health risk assessment of Al, Be, Sb, Sn, Ti and Tl in PM$_{10}$ under different advections of air masses. These metals/semi-metal were studied in samples collected in an area influenced by industrial activities in northern Spain with the aim of analysing the variations in PM$_{10}$ metal/semi-metal. Elemental concentrations were assessed over a period of one year in terms of air mass origin by means of back trajectories (HYSPLIT), the conditional probability function, polar plots, PM concentration roses, aerosol maps (NAAPs) and receptor modelling. The mean concentrations of Al, Be, Sb, Sn, Ti and Tl were 254, 0.02, 1.30, 1.15, 15.3 and 0.20 ng/m^3, respectively, and were within the usual range for suburban stations in Europe. The highest levels were recorded during conditions of regional air mass origin, highlighting the importance of sources not far from the station. Under these circumstances, the renovation of air masses was not produced. The main sources of metals were anthropogenic, mostly related to the use of coal and coke production. In general, the cancer and non-cancer risk values obtained in this study fell within accepted precautionary criteria in all trajectory groups. However, in order to improve air quality and reduce risks to human health, the impact resulting from the joint inhalation of Al, Be, Sb, Sn, Ti and Tl should not be ignored when air masses are fundamentally of regional origin.

© 2019.

1. Introduction

Airborne particulate matter has been classified as group 1 carcinogenic to humans by the International Agency for Research on Cancer (IARC). Heavy metals constitute a significant part of the composition of these particles (Dimitriou and Kassomenos, 2017b; Sun et al., 2014). Al and Tl are metals present in the Earth's crust (ATSDR, 2008; ATSDR, 1992). The average concentration of Tl is generally below 1 ppm (Belzile and Chen, 2017), while Al is the most abundant metal. Fossil fuel combustion (i.e. coal) stands as an important anthropogenic emission source of Al and Tl (Demiray et al., 2012; Chen et al., 2013). Other important anthropogenic sources of Tl are metal smelting and cement production (Demiray et al., 2012; Kazantzis, 2000; Peter and Viraraghavan, 2005). Tl is a constituent of coal and many sulphide ores, and can be partially vaporized in flue gases, reaching concentrations in fly ash 2–10 times higher than in coal. Furthermore, this metal remains in air, water and soil for a long time and does not decompose (López Antón et al., 2013).

Be and Sb also enter the environment as a result of both natural and human activities. Be is present in the atmosphere due to soil resuspension from places where it is enriched (e.g. open-cast mines or near factories processing raw materials with Be) (Bohdalkova et al., 2012; Thorat et al., 2001). Emissions from coal burning have been identified as a relevant source together with the steel industry, smelting, road traffic and waste incineration (Goddard et al., 2016; Sutton et al., 2012). There is general agreement among the scientific community as to the greater influence of traffic in explaining the levels of Sb in the atmosphere (Smichowski, 2008). Mbengue et al. (2014) used this semi-metal as a tracer for brake wear emissions (Matějka et al., 2011). As Sb is used as a catalyst during plastic manufacturing, emissions of this semi-metal have been detected in the surroundings of incineration facilities burning polyethylene terephthalate (Iijima et al., 2009). Sb has also been quantified around refinery plants as a consequence of the combustion of pet-coke (Bosco et al., 2005).

Inorganic tin compounds are found in small amounts in the Earth's crust and the atmospheric presence of Sn is generally caused by anthropogenic activities (Malandrino et al., 2016). Gases, dusts and fumes containing Sn may be released from smelting (Querol et al., 2007) and refining processes, the burning of waste and fossil fuels

* Corresponding author.
Email addresses: negralluis@uniovi.es (L. Negral); bsuarez@uniovi.es (B. Suárez-Peña); eugeniazapicolopez@gmail.com (E. Zapico); fernandezyolanda@uniovi.es (Y. Fernández-Nava); megidolaura@gmail.com (L. Megido); sele.moreno@upct.es (J. Moreno); emara@uniovi.es (E. Marañón); cleonor@uniovi.es (L. Castrillón)

(ATSDR, 2005; Bozkurt et al., 2018), glass-making activities (Ledoux et al., 2017), electronic and mechanical industries (Altintas et al., 2016), coke ovens and other coal processing industries (Khare and Baruah, 2010). This metal is also emitted by traffic (Megido et al., 2016a), being present in road dust (Amato et al., 2009) due to brake abrasion (Minguillón et al., 2013) and probably, to a minor extent, due to tyre abrasion because of the lower amounts of Sn in tyres (Amato et al., 2014).

Ti is defined as a crustal matter species as a consequence of the relative high abundance of mineral oxides (Daher et al., 2012; Guo et al., 2017; Habashi, 2001). Accordingly, its presence in the atmosphere is explained by natural soil resuspension (Negral et al., 2008) or after the abrasion of the road surface (Shirmohammadi et al., 2017). Ti oxide is used as refractory material (Habashi, 2001; McMullen and Faoro, 1997). Powdered Ti is being implemented for aerospace, automotive and other industrial applications (Abkowitz et al., 2011). Powdered titanium carbide is used in the production of hard-alloy tools, carbide steels, abrasive pastes and dispersion-hardened alloys (Onishchenko et al., 2019). In addition to the refractory application, TiO_2 acts as catalyst for chemical/photochemical reactions (Morillas et al., 2019; Nemmar et al., 2013).

These metals and semi-metal present in the inhalable fraction of particulate matter (PM) may cause human health risks. The IARC and the United States Environmental Protection Agency (US EPA) have classified toxic agents according to their weight-of-evidence (WOE) for carcinogenicity in humans (IARC, 2018; US EPA, 2014). Al, Tl, Sb and Sn are not classified by either the IARC or US EPA, although the IARC states that "no determination of non-carcinogenicity or overall safety should be inferred" from this lack of classification (IARC, 2018). Chronic inhalation of antimony trioxide and titanium dioxide is classified by the IARC as 2B: possibly carcinogenic (US EPA, 2014). The US Department of Health and Human Services (DHHS) has determined that Be is a human carcinogen (ATSDR, 2002). The US EPA has determined that Be is a probable human carcinogen. The chronic inhalation of Be compounds has been classified in the categories: 1-carcinogenic (IARC WOE) and LH-likely to be carcinogenic (US EPA WOE) (US EPA, 2014).

The risk for human health caused by these metals/semi-metal is associated with the concentrations in different air masses depending on their origin. Synoptic conditions regulate PM at any locality (Dimitriou and Kassomenos, 2018), not only due to the precipitation associated with some synoptic systems, but also to wind velocity and direction, as well as atmospheric stability (Fonseca-Hernández et al., 2018). Several forecasts have been published highlighting that variations in atmospheric circulation may negatively alter the efficiency of European measures for the abatement of PM (Messori et al., 2018). Moreover, the presence of pollutants in the troposphere may lead to changes in the circulation of air masses. Microphysical interactions among airborne aerosols and other atmospheric pollutants have been reported as the driving force for disruptions observed in model circulation patterns (Fiore et al., 2015). For example, on the Italian coastline of Venice, Masiol et al. (2015) found that certain elements of anthropogenic origin presented a notable inter-correlation in the submicron mode (S, K, Mn, Cu, Fe and Zn) and the intermediate mode, 1-4 μm (Mn, Cu, Zn, Ni). In the latter size, these authors observed a geochemical relationship explained by sea elements (Na, Mg and Cl) and crustal elements (Si, Mg, Ca, Al, Ti and K). Atmospheric circulation increased the anthropogenic elements when winds came from Central and Eastern Europe and from the city of Venice. The concentration of elements in submicron and intermediate modes also increased under low wind velocities and calms. Conversely, strong winds favoured

the increase in the coarse mode: sea aerosol and silica-enriched particles. Papanastasiou and Melas (2009) reported that strong winds from the sea were not necessary to worsen air quality in the coastal city of Volos (Greece). These authors concluded that conditions leading to stagnation, and therefore higher PM10 levels, were frequently found during days with a sea breeze, while ventilation was generally not intense.

Air mass residence time has been used as a predictor variable for PM levels via the implementation of multivariate linear regression (MLR) models (Kavouras et al., 2013). Dimitriou and Kassomenos (2017a) applied the air stress index (PM_{10}, O_3, SO_2, NO_2 and CO) to synoptic systems and airflows in Germany. These authors concluded that the values of said index might have an epidemiological impact of sufficient magnitude to warrant the development of studies with cohorts of the German population. This air stress index, however, did not include any heavy metal. In another study (Dimitriou and Kassomenos, 2017b), they consequently warned about the cancer risk caused by inhaling arsenic in PM_{10} when eastern airflows reached some German cities. A study covering an entire country (Díaz et al., 2017) has already pointed out the relationship between synoptic charts responsible for African dust outbreaks over the Iberian Peninsula and daily mortality in Spain. These studies did not cover the metals studied in the present paper.

To the best of our knowledge, very little research has been published in the scientific literature on the variation in Al, Be, Sb, Sn, Ti and Tl in PM_{10} as a result of atmospheric circulation that also considers the implications for human health. The main objective of this study was the assessment of the anthropogenic sources of Al, Be, Sb, Sn, Ti and Tl present in PM_{10} and the meteorological influences and their implications for human health in an area with historical problems with PM_{10} levels. The results may contribute to helping environmental managers to take measures to prevent the population from being exposed to increased concentrations of pollutants based on the origin of air masses. The following tasks have been performed in this study:

1. Evaluation of the concentrations of Al, Be, Sb, Sn, Ti and Tl present in PM_{10} in terms of atmospheric circulation.
2. Investigation of the origin of the emissions of these six metals/semi-metal in an industrial context.
3. Assessment of the possible risks resulting from the inhalation of these particles for the health of the children and adults living in the sampled area.

2. Methodology

2.1. Description of the location

PM_{10} samples were taken from an industrial suburban station located in Langreo, in an area with historical problems with PM_{10} levels. The sampled area is located in the Nalón Valley, oriented in the northwest-southeast direction, forming part of the 'green' region of the Iberian Peninsula, within the Eurosiberian region, 30 km from Spain's northern shoreline. The area, which has a population of around 3000 inhabitants, has undergone rapid, disorderly industrial development which led to the growth of industrial facilities around existing dwellings. Details on local industrial activity and neighbourhoods are provided in Fig. 1 and the Supplementary Material. Moderate traffic (15 000-25 000 mean vehicles/day) also influenced the station, with the equipment being located 200 m from the AS-117 regional highway (Megido et al., 2017a).
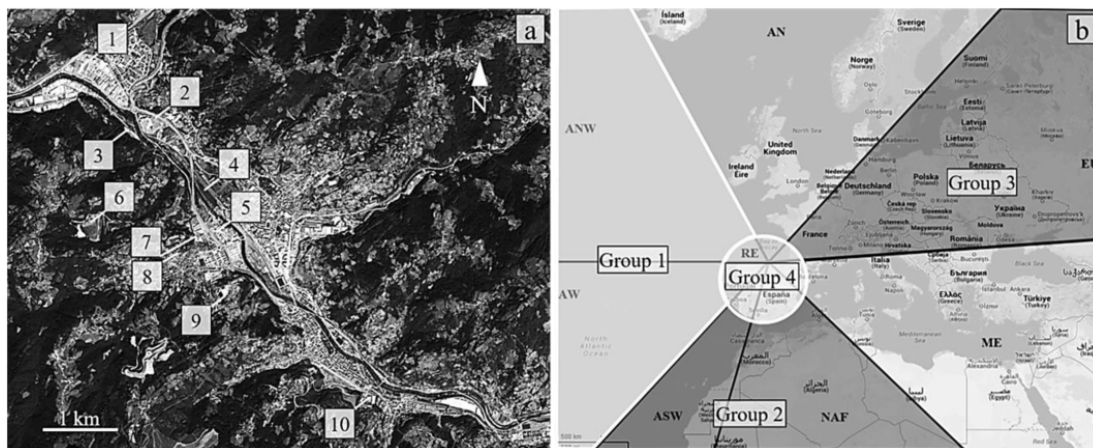
Fig. 1. a) Location of the air pollution sampling station and the main local industries: an industrial hub with a refractory materials factory, an asphalt agglomerate factory and a metal recycling plant (1); a machined and forged parts factory (2); an asphalt plant (3); a coal storage yard (4); a coal-fired power plant (5); a fly ash and slag landfill (6); a metal waste recycling plant (7); the sampling station (8); a factory producing ceramic materials (9); and a coke plant (10). b) Classification of air masses reaching Langreo according to their origin.

2.2. Sample collection and treatment

PM$_{10}$ samples were collected on a daily basis (24 h) from October 26, 2013 to October 26, 2014 using a MCV CAV-A/MSb high-volume sampler (30 m^3/h). A microbalance with 0.01 mg resolution (Mettler Toledo XA105) was used for subsequent gravimetric determination. The sampler was placed on the roof of the sampling station, 3 m above ground level. Glass microfibre (MCV GF1-150) and quartz microfibre (Pallflex-Tissue Quartz 2500QAT-UP) filters, 150 mm diameter, constituted the matrix for particle collection. Quartz microfibre filters were chemically preferred to glass microfibre filters due to the presence of lower amounts of chemical interference (Megido et al., 2016a). Fifty-two samples were collected on the quartz microfibre filters for subsequent chemical analysis, immediately after gravimetric determination. These samples were taken homogeneously distributed over the entire sampling period (one year), covering the four seasons. The quartz microfibre filters were used once a week, rotating the day of the week every new week. The chemical analysis followed were those described in Megido et al. (2016a; 2016b) and comprised 40 analytes including metals/semi-metals, organic and elemental carbon, and inorganic ions. Regarding the quality assurance of the analysis, blank filters and reference material from the National Institute of Standards and Technology, namely Standard Reference Material® 1648a (urban particulate matter), were used as control for the analysis. Errors mostly remained below 10% for the certified elements in the standard. Further details on the analytical determination are provided in the Supplementary Material. The remaining 314 glass microfibre filters were solely used for gravimetric determinations.

2.3. Meteorological scenarios

Fig. 2 shows the wind rose obtained from data recorded by the weather tower at the sampling station. Daily information on maximum wind speed, wind direction and elemental concentration in PM$_{10}$ was used to draw polar plots of the analysed species in PM$_{10}$. The NAAPS Global Aerosol Model and the analysis of five-day isentropic back trajectories (ending at 12:00 UTC) calculated at three heights (750, 1500, 2500 m above sea level) using the HYSPLIT model from NOAA (Stein et al., 2015) were reviewed daily to char-

acterize the air masses. The back trajectories of these air masses reaching the sampling point led to the classification of the masses as Northern Atlantic (AN), North-western Atlantic (ANW), Western Atlantic (AW), South-western Atlantic (ASW), Northern African (NAF), Mediterranean (ME), European (EU) and Regional (RE). This classification (Fig. 1) was based on the air mass trajectories reaching the Iberian Peninsula (Font Tullot, 2000). During these advections, the paths that wind uses to reach a point can be associated with the source of pollutants (Dimitriou and Kassomenos, 2018; Gildemeister et al., 2007; Kavouras et al., 2013). The air mass origins were grouped into four clusters according to their origin and associated pollutant levels. Group 1 includes AN, ANW and AW; this pattern comprises systems that normally reduce the pollution level due to the advection of Atlantic air masses, usually associated with cleaner air conditions (Saavedra et al., 2012). Group 2, which includes ASW and NAF, is associated with the detection of African dust outbreaks that expectedly worsen the atmospheric environment due to mineral contribution from African deserts (Escudero et al., 2006). Group 3 is represented by EU air mass origin, usually resulting in depletion of air quality due to transportation of air pollutants from Central Europe (Megido et al., 2017b). Group 4 comprises only RE and is associated with stagnant conditions that do not facilitate the dispersion of pollutants (Negral et al., 2012). ME air mass origin was not detected during the sampling period.

Another meteorological application of the wind direction is the conditional probability function (CPF). This can be used as a method to estimate the relative frequency or probability that a given condition (e.g. a high score event) occurs in a wind direction. As the relative position of a receptor is important for it to be influenced by a pollution source, this strategy may help to highlight the source (Gildemeister et al., 2007). If the CPF is associated with a feature in a population (e.g. the 90th percentile), events in the upper range of the population will be plotted according to the wind direction. In this paper, the CPF was calculated and plotted for the 90th percentile of PM$_{10}$ and each metal/semi-metal in PM$_{10}$ (Uria-Tellaetxe and Carslaw, 2014). The CPF was mathematically calculated as in Dimitriou and Kassomenos (2017b):
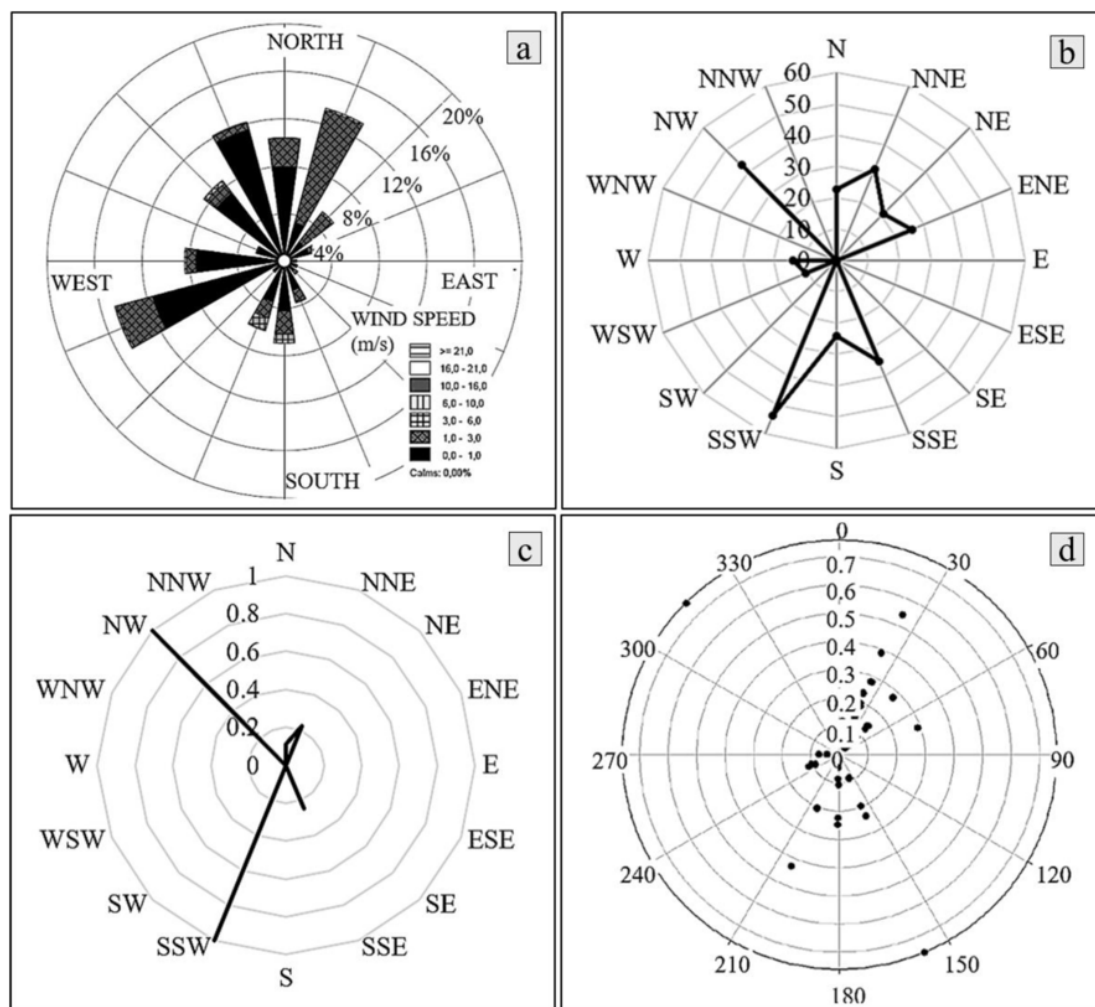
$$CPF_i = \frac{m_i}{n_i} \tag{1}$$

Fig. 2. a) Wind rose at the sampling station from October 26, 2013 to October 26, 2014. b) Mean PM_{10} concentration rose ($\mu g/m^3$) during the sampling period. c) Conditional probability function for PM_{10}. d) Polar plot of Tl (ng/m^3).

where CPF_i is the conditional probability function of a variable in wind sector i; m_i is the number of days when the 90th percentile concentration of a variable (i.e. either PM_{10} or a metal/semi-metal in PM_{10}) was exceeded in wind sector i; and n_i is the total number of days under the same wind direction i.

Wind directions were grouped into 16 wind sectors.

2.4. Receptor model: PCA-MLRA

Principal Components Analysis was used as a statistical tool to reduce the information from 40 analytical variables (including metals, carbon and soluble species, after discarding ten other analytical variables) to a lower number of independent factors. The distance between factors was broadened by Varimax rotation. Each of the former 40 variables presented robust values of concentration during 52 days, each PM_{10} sample being taken over a period of 24 h. Reviewing the factor loadings for each factor, chemical tracers allowed each independent factor to be associated with either a source or a recognized pattern for aerosols. After identifying the source/factor, a multiple lineal regression analysis (MLRA) was implemented considering the identified factors/sources as regressors and PM_{10} or a chemical

species as the dependent variable. The model was run using the Statistica software as explained elsewhere (Megido et al., 2017b).

2.5. Human health risk assessment

The model used to calculate human exposure to PM_{10} metals/semi-metal was based on those developed by the US EPA. The following assumptions underlie the model applied in this study: 1) the potential receptors of metal particles suspended in the air were the residents living in the sampled area; 2) the target subjects were divided in two groups, namely children (≤6 years) and adults (≥21 years) (US EPA, 2014); 3) the analysed via of exposure was inhalation; and 4) no characteristic population parameters for local residents or exposure characteristic parameters from the location under study were found. Standard default values were used in the calculation.

The numerical expressions used in the calculations of the inhalation exposure concentration (EC_{inh}), inhalation cancer risk (CR_{inh}) and inhalation non-cancer risk (HQ_{inh}) were based on those developed by the US EPA (2009). The US EPA inhalation dosimetry methodology was based on the EC_{inh}. The methodology assumes that EC_{inh} is directly related to airborne metal concentration (C_{air}). Due to the uncertainty associated with the C_{air} estimate, we used the 95% up-

per confidence limit (UCL) on the arithmetic mean metal PM_{10} chosen as the exposure point concentration. (US EPA, 1989). EC_{inh} was calculated for each of the six metals/semi-metal in each air mass group, according to the following expression (US EPA, 2009).

$$EC_{inh} = C_{air} \cdot ET \cdot \frac{EF \cdot ED}{AT} \; (\mu g \cdot m^{-3}) \quad (2)$$

where ET represents exposure time (24 h/day); EF, exposure rate (350 days/year for local residents); ED, exposure duration (the recommended default values of US EPA (2014) were used, i.e. 6 years for children and 20 years for adults); and AT is the averaging time (for carcinogens, $AT = 70$ years $\bullet$ 365 day/year $\bullet$ 24 h/day and for non-carcinogens, $AT = ED \bullet$ 365 day/year $\bullet$ 24 h/day).

Once the exposure had been assessed, the CR_{inh} and HQ_{inh} were analysed, the latter via the calculation of the Hazard Quotient (HQ) (US EPA, 1989; 2009):

$$CR_{inh} = IUR \cdot EC_{inh} \quad (3)$$

$$HQ_{inh} = \frac{EC_{inh}}{RfCi \cdot 1000 \; \mu g/mg} \quad (4)$$

where IUR represents Inhalation Unit Risk, $2.4 \bullet 10^{-3} \; (\mu g \bullet m^{-3})^{-1}$ for Be (US EPA, 2017); and RfC_i, Inhalation Reference Concentrations.

RfC_i values for Al, Be, Sb and Ti were $5 \cdot 10^{-3}$, $2 \cdot 10^{-5}$, $2 \cdot 10^{-4}$ and $1 \cdot 10^{-4}$ mg/m^3, respectively (US EPA, 2017). Sb and Ti were assumed to be present as Sb (trioxide) and Ti (tetrachloride), respectively. Ferreira-Batista et al. (2005) and Keshavarzi et al. (2015) considered that, once the particles were inhaled, the absorption of their toxins had similar effects on human health to those caused by their ingestion. Accordingly, as RfC_i data on Sn and Tl were not found, they were replaced by oral reference doses (RfD_o) of Sn and Tl (oxide): $6 \cdot 10^{-1}$ and $2 \cdot 10^{-5}$ mg/(kg$\bullet$day), respectively (US EPA, 2017; Sun et al., 2014).

3. Results and discussion

3.1. Composition of PM_{10}: Al, Be, Sb, Sn, Ti and Tl

The mean concentration of PM_{10} during the sampling period was 20 $\mu g/m^3$, which is the current annual mean guideline PM_{10} concentration established by the World Health Organization (WHO, 2005). The number of days above 50 $\mu g/m^3$ was 11, which is below the European Union threshold (35 days per year). The daily values are presented in the Supplementary Material (Fig. S2). Table 1 presents the concentrations of Al, Be, Sb, Sn, Ti and Tl in PM_{10}. The mean concentration of Al was nearly twice the value determined by Megido et al. (2016b) at a suburban traffic-oriented station in Gijón, a coastal city 30 km from Langreo, namely 132 ng/m^3. The contribution from local industry, including the handling of bulk materials, may explain this difference. Limbeck et al. (2009) published the Al content at urban stations with different traffic intensity in Vienna. These authors obtained annual mean values ranging from 570 to 340 ng/m^3, traffic being responsible for the upper extreme of the range.

The mean concentrations of the other elements were 1-5 orders of magnitude below the annual mean concentration of Al, with Be constituting the scarcest species. Be concentration remained below the levels recorded at stations on the Iberian Peninsula in a similar context: for urban background stations (0.02–0.05 ng/m^3) or industrial

stations influenced by building material activities such as glaze and ceramic tile (0.02–0.05 ng/m^3), and brick manufacturing (0.07 ng/m^3) (Querol et al., 2007). This overview can be compared with suburban industrial stations across the United Kingdom ($32 \cdot 10^{-3}$-$4 \cdot 10^{-3}$ ng/m^3) (Goddard et al., 2016).

Sb presented a similar concentration to that found at the suburban station on the shoreline: 1.1 ng/m^3 (Megido et al., 2016a). In the aforementioned study, the influence of traffic was proven by correlations and ratios of traffic tracers such as Sb. In the present study, the Cu/Sb ratio reached a value of 5.4, in line with the ratio of 7.0 ± 1.9 published by Amato et al. (2009). At a similar monitoring station located 150 km east of Langreo, a concentration of 1.8 ng Sb/m^3 was obtained at a point influenced by industrial activity and traffic (Fernández-Olmo et al., 2016). All these values for the northern Iberian Peninsula fall within the lowest extreme of the range for similar stations in Europe (Amato et al., 2016). Sb is predominantly emitted by traffic (Matějka et al., 2011), low levels signifying the ameliorated impact of traffic at the station.

The mean Sn concentration in Langreo was also low, particularly when compared with traffic-oriented stations, e.g. up to 34 ng/m^3 in Milan (Amato et al., 2016). This finding supports the idea of the scant influence of traffic at the sampling point.

As Ti is a crustal species (Guo et al., 2017), it was not surprising that it ranked as the second most abundant element of the six. The concentration fell within the range of other urban/suburban studies in Spain, 18–83 ng/m^3 (Querol et al., 2007), and Europe, 13.7–30.2 ng/m^3 (Amato et al., 2016). In the study by Megido et al. (2016a), the Al/Ti ratio was nearly the same as in this paper (around 17). A similar ratio endorses the hypothesis of common behaviour for both metals. The Al/Sb ratio was found to be 120 in Megido et al. (2016a) and 195 in this study. This difference points to an unequal pattern for Sb, a traffic tracer (Shirmohammadi et al., 2017), compared to Al and Ti. The latter elements are also traffic tracers due to road surface abrasion and subsequent road dust resuspension. It can thus apparently be concluded that traffic was not so intense at the Langreo station, as it did not interfere in non-exhaust emissions.

Despite the fact that the sampling station is close to different industrial facilities, Tl only reached 0.2 ng/m^3. Nevertheless, the mean concentration in Langreo was once again double to that recorded in Gijón (0.1 ng Tl/m^3) (Megido et al., 2016a). This confirmed the anthropogenic influence of this metal in the local atmosphere, as it was above the usual level for rural backgrounds (0.1 ng/m^3), remaining in the reported range for urban backgrounds (0.05-0.4 ng/m^3) (Querol et al., 2007). The main influence was probably due to coal combustion to the detriment of other sources such as traffic. Nearly 2 ppm were detected in fly ash by Lieberman et al. (2016), while Tl was not generally detected in road dusts (Amato et al., 2014).

3.2. Chemical factorization and source apportionment

Eight factors were extracted after the PCA, explaining 80.4% of the variance of the data. The eight factors were associated with the following sources (Fig. S1): coal combustion (30.7% contribution to PM_{10}); ceramic and building materials industry (3.5%); metallurgy (0.7%); coke industry (19.5%); secondary aerosol (27.9%); marine aerosol (6.1%); mineral and bitumen industry (2.9%); and traffic (8.7%).

The contribution of coal combustion and coke production was above half the overall contribution of PM_{10}. Simultaneously, any one of these sources comprised the first contribution of the six elements, with the exception of the semi-metal (Fig. S1). The factor loadings of chemical species and the values observed and predicted by the model

Table 1

Elemental concentrations and health risk assessment for Al, Be, Sb, Sn, Ti and Tl in PM10 at the Langreo sampling station according to air mass origin. Group 1: AN, ANW and AW; Group 2: ASW, and NAF; Group 3: EU; and Group 4: RE. LCL stands for a 5% confidence limit, and UCL for a 95% upper confidence limit. The calculated health risk values are: inhalation non-cancer risk (HQ_{inh}), inhalation cancer risk (CR_{inh}) and the hazard index (HI).

Group		Value		Element						HI
				Al	Be	Sb	Sn	Ti	Tl	
1	Metal conc. (n=31)	Min.		14.1	<0.01	0.08	0.07	1.22	0.03	
		LCL		26.6	<0.01	0.09	0.15	2.04	0.03	
		Mean		173	0.01	0.96	0.95	10.8	0.16	
		UCL		380	0.02	2.46	2.27	36.8	0.41	
		Max.		609	0.06	4.03	3.17	53.5	0.47	
		HQ_{inh}	children	7.29E-02	1.12E-03	1.18E-02	3.63E-06	3.53E-01	1.95E-02	4.58E-01
			adults	7.29E-02	1.12E-03	1.18E-02	3.63E-06	3.53E-01	1.95E-02	4.58E-01
		CR_{inh}	children		3.95E-09					
			adults		1.31E-08					
2	Metal conc. (n=3)	Min.		143	<0.01	0.39	0.70	7.03	0.04	
		LCL		143	<0.01	0.39	0.70	7.03	0.04	
		Mean		267	<0.01	0.63	0.99	23.4	0.18	
		UCL		371	0.02	0.92	1.38	43.8	0.25	
		Max.		371	0.02	0.92	1.38	43.8	0.25	
		HQ_{inh}	children	7.12E-02	7.29E-04	4.42E-03	2.21E-06	4.20E-01	1.20E-02	5.08E-01
			adults	7.12E-02	7.29E-04	4.42E-03	2.21E-06	4.20E-01	1.20E-02	5.08E-01
		CR_{inh}	children		3.95E-09					
			adults		1.31E-08					
3	Metal conc. (n=4)	Min.		67.1	<0.01	0.50	1.09	7.18	0.09	
		LCL		67.1	<0.01	0.50	1.09	7.18	0.09	
		Mean		208	0.01	1.39	1.28	12.7	0.18	
		UCL		286	0.02	2.39	1.65	18.0	0.28	
		Max.		286	0.02	2.39	1.65	18.0	0.28	
		HQ_{inh}	children	5.48E-02	9.45E-04	1.15E-02	2.64E-06	1.73E-01	1.32E-02	2.53E-01
			adults	5.48E-02	9.45E-04	1.15E-02	2.64E-06	1.73E-01	1.32E-02	2.53E-01
		CR_{inh}	children		3.95E-09					
			adults		1.31E-08					
4	Metal conc. (n=14)	Min.		8.45	<0.01	0.34	0.58	5.25	0.07	
		LCL		8.46	<0.01	0.40	0.59	5.34	0.08	
		Mean		444	0.03	2.18	1.57	24.4	0.31	
		UCL		1.53E+03	0.12	6.73	4.16	70.1	0.76	
		Max.		1.57E+03	0.14	6.78	4.64	70.6	0.76	
		HQ_{inh}	children	2.94E-01	5.71E-03	3.23E-02	6.65E-06	6.72E-01	3.64E-02	**1.04**
			adults	2.94E-01	5.71E-03	3.23E-02	6.65E-06	6.72E-01	3.64E-02	**1.04**
		CR_{inh}	children		2.37E-08					
			adults		7.89E-08					
	Metal conc. (all days, n=52)	Min.		8.45	<0.01	0.08	0.07	1.22	0.03	
		LCL		15.3	<0.01	0.17	0.24	2.12	0.03	
		Mean		254	0.02	1.30	1.15	15.3	0.20	
		UCL		773	0.05	4.02	2.27	52.5	0.54	
		Max.		1.57E-03	0.14	6.78	4.64	70.6	0.76	

Units: metals/semi-metal concentration (ng/m^3).

are provided in the Supplementary Material (Table S1 and Fig. S2). The first factor, F1, explained 34.0% of the variance of data, with As, OC, EC, Pb, Cd and Sn presenting the highest factor loadings. Fig. S1 shows that F1 explained more than half of the concentrations of Ti and Tl, these elements being associated with coal (Chen et al., 2013; Steinmetz et al., 1988). From Fig. 2, the impacting directions of Tl can be seen to be NE (0-45°) and W and NW, the last with infrequent events. A coal-fired power station is located 0.5 km NNE, with a coal fly ash/slag landfill 1 km to the NW. A residential borough SW of the station contains dwellings burning coal as their heating system. The relevance of these directions is shown on the graph of the CPF in Fig. 2. For these reasons, it was proposed to associate F1 with coal combustion.

The second factor, F2, accounted for 10.1% of the variance. The highest factor loadings were observed for La, Ce, Zr, Cr and Ti. These elements are related to emissions during the production of ceramic materials, most of which are of crustal origin (Minguillón et al. (2013); Rudnick and Gao (2003); Vikulin et al. (2004); Nath et al. (2018). It should be noted that coal fly ash may be used as a raw ma-

terial during the processing of building materials, e.g. concrete (Lieberman et al., 2018). There were facilities manufacturing refractory products, ceramic materials, mortar and concrete 0.6 km NE of the station. A series of facilities belonging to the ceramic, stonework and building materials industry were based at 315-325°. These facilities stored bulk materials in open yards which were used to produce dry mortar, concrete and cement, among other such materials. The topography of the valley meant that pollutants from these activities reached the sampling station from the NE. The factory producing ceramic materials, situated SE of the station, helped to explain the situation due to its use of bentonite and kaolin as raw materials.

The third factor, F3, accounted for 9.1% of the variance. The elements with the highest factor loadings were Zn, F, Mn, Bi and Mg. Scrapyards and metallic carpentry workshops may account for the presence of these metals (Chicharro et al., 1998; Westfall et al., 2016; Fuge, 2019; Di and Zhuang, 2010; Shang et al., 2012). There was a scrapyard 0.12 km NNE of the sampling station, with mechanized steel workshops located a little further away in the same direction. Two other metal recycling facilities were located on an industrial es-

tate at a distance of 2.7 km, 315-325° from the station, although their emissions reached the station from the NE due to the local topography. Metallic carpentry workshops, entailing welding and oxy-cutting, were situated to the south of the station, which could explain the influence on F3.

The fourth factor, F4, explained 7.7% of the variance. Al, Sr, Ba, Ti, Be, Li, K, La, Ce, Fe, Ta, Tl, V, Co and the carbonaceous fraction had factor loadings above 0.4. Many of these elements are mineral in nature (Pey et al., 2013) and may be associated with mineral phases present in coal (Querol et al., 1996; Lieberman et al., 2018). There was a coke plant SE of the station. The plant employed hard coal to produce coke as a raw material. Fe, Ca, Al, K, Ba, Sr, Co and V are elements present in PM emitted during coke production (Tsai et al., 2007; Konieczynski et al., 2012; Hedberg et al., 2005). For these reasons, F4 was defined as coke industry.

The fifth factor, F5, supposed 5.7% of the variance. The secondary inorganic compounds SO_4^{2-}, NH_4^+ and NO_3^- were the species with the highest factor loadings. All these substances have been previously included in factors known as secondary aerosol (González-Castanedo et al., 2015).

The sixth factor, F6, comprised 5.2% of the variance. Na, Mg, Cl^- and, to a lesser extent, Ni were the species with the highest factor loadings. The first three elements are tracers of marine aerosol (Megido et al., 2017b), whereas the last would not be of natural origin. During days with an important contribution from this factor, the V/Ni ratio was two orders of magnitude (up to 0.07) lower than that from the Earth's crust (2.06) (Rudnick and Gao, 2003). At the same time, the Cl/Na ratio (2.1) was similar to that of sea water (Zapico López, 2015). Consequently, it may be posited that Ni was brought by marine air masses transporting ship emissions from oil combustion (Viana et al., 2014). For all the above reasons, F6 was proposed to be defined as marine aerosol.

The seventh factor, F7, explained 3.9% of the variance. Three elements had high factor loadings: Rb, Sb and Ta. The association with mineral-crustal elements (e.g. Li, Al, Ba, Sr and Ti) was found to a certain extent in F7. As to airborne Sb, apart from brake pads, the sources of this pollutant have also been attributed to combustion (González-Castanedo et al., 2015). This was in keeping with the detection of V and Ni in F7; in fact, these elements were found in road asphalt containing bitumen (Hedberg et al., 2005). The presence of the high factor loading of Ta, a high field strength element, was difficult to interpret. Nonetheless, it may be attributed, on the one hand, to Sn mining and scrap (Filella, 2017; Sánchez-Rodas et al., 2017) and, on the other, to the influence of intense traffic (Querol et al., 2004).

There was an industrial plant manufacturing asphalt aggregate 2.8 km NE of the sampling station. The process consumed aggregates of calcium, silica, bitumen and cement as raw materials as well as fuel oil and gasoil to produce heat. F7 presented its maximum peak on June 23, 2014, when dust from the African desert had been penetrating the area for some days. This situation may cautiously suggest F7 to be a factor influenced by the asphalt aggregate industry and mineral contribution.

The eighth factor, F8, explained 3.2% of the variance. Fe, Cu, Sn and Ca were elements with notable factor loadings. Fe, Ca, Al and Mg form part of the crustal matter related to traffic due to road dust resuspension (Karanasiou et al., 2011). Zn was released into the atmosphere by tyre abrasion, whereas Ba, Cu and Sb were released due to brake wear (Moreno et al., 2011). OC, EC, Mo, Ce and NO_3^- (resulting from nitrogen oxides) can be listed among the exhaust emissions of internal combustion engine vehicles (Karanasiou et al., 2011). On the basis of the tracers and weak pattern detected in F8, which decreased on weekends, this factor may be proposed as traffic.

3.3. Meteorological scenarios

According to the information provided in Table 1 and Fig. S3, all extreme values for the metals/semi-metal appeared under regional air masses (Group 4), with a lack of intense ventilation. In line with this finding, low ventilation rates were shown to be less efficient in removing ultrafine particles (Kylafis et al., 2019). This is not surprising for crustal elements like Al, which may originate from wind-blown soil dust and resuspension of soil dust, (Khare and Baruah, 2010). However, Langreo is a wet area with broad-ranging plant coverage, where the resuspension of natural soils would be limited. This situation highlights the importance of sources across the local valley during pollution episodes. The minimum levels for metals/semi-metal were recorded under the influence of Group 1 air masses. This was to be expected, as Atlantic air masses are assumed to be cleaner than local emissions (Saavedra et al., 2012). The levels of metals/semi-metal also decrease in the event of air masses directly reaching the sampling point via the 30 km trajectory from the coast and in the presence of rainfall. Variable amounts of rainfall (from 0.4 to 9.5 mm) were detected on the days with minimum concentrations of metals/semi-metal. Intense advections from Group 2 and 3 air mass origins increased the concentrations of the six elements in the lower part of the range (i.e. minimum and lower confidence limit, LCL), while the concentrations of the six elements were lower in the upper extreme of the range (i.e. UCL, upper confidence limit, and maximum). This observation would mean that powerful drags from Africa or Europe would slightly increase levels of pollutants, acting as a background increase. This is agreement with Al, a tracer of African dust outbreaks (Querol et al., 2019), which clearly increased the minimum and LCL concentrations by two orders of magnitude when considering North African air masses instead of all air mass origins. However, the presence of advections from Groups 2 and 3 was not as important in peak pollution events as regional air masses, Group 4. In summary, the importance of meteorology was greater than that of the sources around the station. This is agreement with the conclusions published by Sutton et al. (2012), who observed that airborne Be was preferentially correlated with local weather patterns and PM_{10}, rather than with operational activities.

3.4. Health risk assessment

Table 1 shows the values for HQ_{inh} and CR_{inh} and the hazard index (HI) corresponding to backward trajectory groups for Al, Be, Sb, Sn, Ti and Tl in PM_{10}.

As stated in the Introduction, the IARC classifies Be as Group 1, carcinogenic; and Sb_2O_3 and TiO_2 as Group 2B, possibly carcinogenic. Al, Tl and Sn are not classified by the IARC. In this paper, carcinogenic risks were only assessed for those elements whose inhalation unit risk (IUR) has already been established by the US EPA. This is the case of Be. The carcinogenic risk levels in children and adults for this metal were $<10^{-6}$, with higher values for adults than for children (Table 1). Thus, carcinogenic risks for Be were lower than the internationally accepted precautionary criterion (10^{-4}-10^{-6}), indicating that the carcinogenic risk posed by Be via inhalation is acceptable in Langreo for both children and adults, for all trajectory groups.

With respect to non-carcinogenic risks, the HQ_{inh} of single metals (Al, Be, Sb, Sn, Ti and Tl) via inhalation was below the safe level of 1 for both subpopulations under study, in all trajectory groups (Table 1). This indicates no non-carcinogenic risk from inhalation exposure for each single element. For children and adults, the HQ_{inh} of Ti under the influence of Group 4 air masses was the highest ($6.72 \cdot 10^{-1}$).

As expected, the HQ_{inh} for Ti increased in the regional trajectory group. This endorsed the hypothesis of the importance of emitting sources of this element not far from the sampling station (i.e. coal combustion or the coke plant, Fig. S1). As regard the HQ_{inh} for Al, the determined values were of the same order of magnitude as those calculated by Brown et al. (2015) on one of the most highly trafficked roads in Manchester.

The hazard index (HI) is equal to the sum of multiple-chemical or multiple-route HQ (US EPA, 2009). If the HI value is greater than 1, this shows that there is a chance that non-carcinogenic effects may occur. Thus, the greater the HI value, the higher the probability of non-carcinogenic effects (US EPA, 2001). HI values for those toxic elements were lower than 1, except the HI values for Group 4 air masses, which were slightly higher (1.04). Comparing the HI values of the backward trajectory groups, HI-Group 4 is approximately 50% higher than HI-Groups 1 and 2, and 76% higher than HI-Group 3. This means that the non-carcinogenic risk arose under circulation types ending in recirculation of air masses (i.e. regional air masses). Under these circumstances, the renovation of air masses was not produced and the accumulation of Al, Be, Sb, Sn, Ti and Tl worsened air quality. Conversely, powerful advections helped to preserve a cleaner atmosphere, regardless of their origin. The drag of fresh marine air masses contributed to maintaining a healthier atmosphere in terms of the non-carcinogenic risks caused by the aforementioned elements.

In the main, the health risks were assessed following a series of assumptions and estimations. There were uncertainties in the estimations of the exposure parameters and metal toxicity data, among others. On the one hand, there are no specific parameters for calculating the exposure of residents in the locality under study. Consequently, the standard default values from the US EPA were adopted. On the other hand, there are uncertainties associated with the metal/semi-metal toxicity data. In other words, total concentrations of the elements were analysed (e.g. Sb, Ti and Tl were measured as total Sb, Ti and Tl, instead of as Sb (trioxide), Ti (tetrachloride) and Tl (oxide), although the latter were assumed in the calculations). Moreover, toxicity related to the joint presence of these metals/semi-metal cannot be dismissed (Wu et al., 2016). Six metals/semi-metal present in PM_{10} were considered, although residents (children and adults) may have been exposed to other potentially toxic elements (Megido et al., 2017a).

4. Conclusions

Heavy metals in airborne particulate matter (Al, Be, Sb, Sn, Ti and Tl) in an inhabited industrial suburban area of northern Spain were studied. Air pollution and meteorological data were combined to assess the potential associated human risks.

The main conclusions of the study are:

− The mean concentrations of the elements are within the usual range for suburban stations in Europe.
− The main sources of metals were anthropogenic in nature, being mostly related to the use of coal and coke production.
− The highest pollutant levels occur under the influence of regional air masses, with poor renovation conditions. Under these circumstances, the mean Al concentration was 444 ng/m^3, the mean concentrations of the other metals being considerably lower, ranging from 0.03 to 24.4 ng/m^3 for Be and Ti, respectively.
− Back trajectory air masses associated with intense advections reduced the levels of pollutants, particularly in the case of Atlantic air masses. The drag of fresh marine air masses contributed to maintaining a healthier atmosphere.

− In general, cancer and non-cancer risk values were below the accepted precautionary criteria (10^{-4} and 1, respectively) for both sub-populations under study, i.e. children and adults, in all trajectory groups. However, the accumulative non-cancer risk was not negligible when regional air masses prevailed.

The results obtained in the present study may contribute to the understanding of the potential risks associated with the inhalation of airborne particulates in suburban environments. Environmental managers could use these findings to prevent residents from being exposed to increased concentrations of pollutants based on the origin of air masses.

Declaration of competing interest

None.

Appendix A. Supplementary data

Supplementary data to this article can be found online at https://doi.org/10.1016/j.chemosphere.2019.125347.

References

Amato, F., Pandolfi, M., Viana, M., Querol, X., Alastuey, A., Moreno, T., 2009. Spatial and chemical patterns of PM10 in road dust deposited in urban environment. Atmos. Environ. 43, 1650–1659. https://doi.org/10.1016/j.atmosenv.2008.12.009.

Amato, F., Alastuey, A., De La Rosa, J., Sánchez De La Campa, A.M., Pandolfi, M., Lozano, A., Contreras González, J., Querol, X., 2014. Trends of road dust emissions contributions on ambient air particulate levels at rural, urban and industrial sites in southern Spain. Atmos. Chem. Phys. 14, 3533–3544. https://doi.org/10.5194/acp-14-3533-2014.

Amato, F., Alastuey, A., Karanasiou, A., Lucarelli, F., Nava, S., Calzolai, G., Severi, M., Becagli, S., Gianelle, V.L., Colombi, C., Alves, C., Custódio, D., Nunes, T., Cerqueira, M., Pio, C., Eleftheriadis, K., Diapouli, E., Reche, C., Minguillón, M.C., Manousakas, M.-I., Maggos, T., Vratolis, S., Harrison, R.M., Querol, X., 2016. AIRUSE-LIFE+: a harmonized PM speciation and source apportionment in five southern European cities. Atmos. Chem. Phys. 16, 3289–3309. https://doi.org/10.5194/acp-16-3289-2016.

ATSDR, 2002. Toxicological Profile for Beryllium. Department of Health and Human Services, Public Health Service Agency for Toxic Substances and Disease Registry, Atlanta, GA, US.

Brown, A., Barrett, J.E.S., Robinson, H., Potgieter-Vermaak, S., 2015. Risk assessment of exposure to particulate output of a demolition site. Environ. Geochem. Health 37, 675–687. https://doi.org/10.1007/s10653-015-9747-3.

Chen, Y.H., Wang, C.L., Liu, J., Wang, J., Qi, J.Y., Wu, Y.J., 2013. Environmental exposure and flux of thallium by industrial activities utilizing thallium-bearing pyrite. Sci. China Earth Sci. 56, 1502–1509. https://doi.org/10.1007/s11430-013-4621-6.

Chicharro, A., Cala, V., Larrea, M.T., 1998. Contamination by heavy metals in soils in the neighbourhood of a scrapyard of discarded vehicles. Sci. Total Environ. 212, 145–152. https://doi.org/10.1016/S0048-9697(98)00007-2.

Di, W., Zhuang, L., 2010. A new Pb-free machinable austenitic stainless steel. J. Iron Steel Res. Int. 17, 59–63. https://doi.org/10.1016/S1006-706X(10)60046-5.

Díaz, J., Linares, C., Carmona, R., Russo, A., Ortiz, C., Salvador, P., Trigo, R.M., 2017. Saharan dust intrusions in Spain: health impacts and associated synoptic conditions. Environ. Res. 156, 455–467. https://doi.org/10.1016/j.envres.2017.03.047.

Dimitriou, A.D., Kassomenos, I., 2017a. The covariance of air quality conditions in six cities in Southern Germany - the role of meteorology. Sci. Total Environ. 574, 1611–1621. https://doi.org/10.1016/j.scitotenv.2016.08.200.

Dimitriou, A.D., Kassomenos, I., 2017b. Airborne heavy metals in two cities of North Rhine. Chemosphere 186, 78–87. https://doi.org/10.1016/j.chemosphere.2017.07.138.

Dimitriou, A.D., Kassomenos, I., 2018. A meteorological analysis of PM10 episodes at a high altitude city and a low altitude city in central Greece – the impact of wood burning heating devices. Atmos. Res. 214, 329–337. https://doi.org/10.1016/j.atmosres.2018.08.014.

Escudero, M., Stein, A., Draxler, R.R., Querol, X., Alastuey, A., Castillo, S., Avila, A., 2006. Determination of the contribution of northern Africa dust source areas to PM10 concentrations over the central Iberian Peninsula using the Hybrid Single-Particle Lagrangian Integrated Trajectory model (HYSPLIT) model. J. Geophys. Res.-Atmos. 111, D06210https://doi.org/10.1029/2005JD006395.

Fernández-Olmo, I., Andecochea, C., Ruiz, S., Fernández-Ferreras, J.A., Irabien, A., 2016. Local source identification of trace metals in urban/industrial mixed land-use areas with daily PM10 limit value exceedances. Atmos. Res. 171, 92–106. https://doi.org/10.1016/j.atmosres.2015.12.010.

Ferreira-Baptista, L., De Miguel, E., 2005. Geochemistry and risk assessment of street dust in Luanda, Angola: a tropical urban environment. Atmos. Environ. 39, 4501–4512. https://doi.org/10.1016/j.atmosenv.2005.03.026.

Filella, M., 2017. Tantalum in the environment. Earth Sci. Rev. 173, 122–140. https://doi.org/10.1016/j.earscirev.2017.07.002.

Fiore, A.M., Naik, V., Leibensperger, E.M., 2015. Air quality and climate connections. J. Air Waste Manag. Assoc. 65, 645–685. https://doi.org/10.1080/10962247.2015.1040526.

Fonseca-Hernández, M., Tereshchenko, I., Mayor, Y.G., Figueroa-Montaño, A., Cuesta-Santos, O., Monzón, C., 2018. Atmospheric pollution by PM10 and O3 in the Guadalajara metropolitan area, Mexico. Atmosphere 9, 243. https://doi.org/10.3390/atmos9070243.

Font Tullot, I., 2000. In: Climatología de España y Portugal, Segunda. Ediciones Universidad Salamanca, Salamanca.

Fuge, R., 2019. Fluorine in the environment, a review of its sources and geochemistry. Appl. Geochem. 100, 393–406. https://doi.org/10.1016/j.apgeochem.2018.12.016.

Gildemeister, A.E., Hopke, P.K., Kim, E., 2007. Sources of fine urban particulate matter in Detroit, MI. Chemosphere 69, 1064–1074. https://doi.org/10.1016/j.chemosphere.2007.04.027.

Goddard, S.L., Brown, R.J.C., Ghatora, B.K., 2016. Determination of beryllium concentrations in UK ambient air. Atmos. Environ. 147, 320–329. https://doi.org/10.1016/j.atmosenv.2016.10.018.

González-Castanedo, Y., Sanchez-Rodas, D., Sánchez de la Campa, A.M., Pandolfi, M., Alastuey, A., Cachorro, V.E., Querol, X., de la Rosa, J.D., 2015. Arsenic species in atmospheric particulate matter as tracer of the air quality of Doñana Natural Park (SW Spain). Chemosphere 119, 1296–1303. https://doi.org/10.1016/j.chemosphere.2014.09.093.

Guo, Y., Gao, X., Zhu, T., Luo, L., Zheng, Y., 2017. Chemical profiles of PM emitted from the iron and steel industry in northern China. Atmos. Environ. 150, 187–197. https://doi.org/10.1016/j.atmosenv.2016.11.055.

Hedberg, E., Gidhagen, L., Johansson, C., 2005. Source contributions to PM10 and arsenic concentrations in Central Chile using positive matrix factorization. Atmos. Environ. 39, 549–561. https://doi.org/10.1016/j.atmosenv.2004.11.001.

IARC, 2018. Agents Classified by the IARC Monographs, Volumes 1-120. Last Update: February 2018. IARC Monographs on the Evaluation of Carcinogenic Risks to Humans. International Agency for Research on Cancer, France. World Health Organization http://monographs.iarc.fr/ENG/Classification/.
, .

Karanasiou, A., Moreno, T., Amato, F., Lumbreras, J., Narros, A., Borge, R., Tobías, A., Boldo, E., Linares, C., Pey, J., Reche, C., Alastuey, A., Querol, X., 2011. Road dust contribution to PM levels - evaluation of the effectiveness of street washing activities by means of positive matrix factorization. Atmos. Environ. 45, 2193–2201. https://doi.org/10.1016/j.atmosenv.2011.01.067.

Kavouras, I.G., Lianou, M., Chalbot, M.C., Vei, I.C., Kotronarou, A., Hoek, G., Hameri, K., Harrison, R.M., 2013. Quantitative determination of regional contributions to fine and coarse particle mass in urban receptor sites. Environ. Pollut. 176, 1–9. https://doi.org/10.1016/j.envpol.2013.01.004.

Keshavarzi, B., Tazarvi, Z., Rajabzadeh, M.A., Najmeddin, A., 2015. Chemical speciation, human health risk assessment and pollution level of selected heavy metals in urban street dust of Shiraz, Iran. Atmos. Environ. 119, 1–10. https://doi.org/10.1016/j.atmosenv.2015.08.001.

Khare, P., Baruah, B.P., 2010. Elemental characterization and source identification of PM2.5 using multivariate analysis at the suburban site of North-East India. Atmos. Res. 98, 148–162. https://doi.org/10.1016/j.atmosres.2010.07.001.

Konieczynski, J., Zajusz-Zubek, E., Jabonska, M., 2012. The release of trace elements in the process of coal coking. Sci. World J. 294927. https://doi.org/10.1100/2012/294927.

Kylafis, G.F., Sleigh, P.A., Tomlin, A.S., Ding, Y., 2019. Evacuation characteristics of released airborne TiO2 nanomaterial particles under different ventilation rates in a confined environment. J. Environ. Manag. 233, 417–426. https://doi.org/10.1016/j.jenvman.2018.12.063.

Lieberman, R.N., Querol, X., Moreno, N., Mastai, Y., Cohen, H., 2016. Physical and chemical changes in coal fly ash during acidic or neutral wastes treatment, and its' effect on the fixation process. Fuel 184, 69–80. https://doi.org/10.1016/j.fuel.2016.06.107.

Lieberman, R.N., Knop, Y., Querol, X., Moreno, N., Muñoz-Quirós, C., Mastai, Y., Anker, Y., Cohen, H., 2018. Environmental impact and potential use of coal fly ash andsub-economical quarry fine aggregates in concrete. J. Hazard Mater. 344, 1043–1056. https://doi.org/10.1016/j.jhazmat.2017.11.047.

Limbeck, A., Handler, M., Puls, C., Zbiral, J., Bauer, H., Puxbaum, H., 2009. Impact of mineral components and selected trace metals on ambient PM10 concentrations Atmos. Environ. Times 43, 530–538. https://doi.org/10.1016/j.atmosenv.2008.10.012.

Matějka, S., Lu, Y., Matějková, P., Smetanad, B., Kukutschová, J., Vaculíka, M., Tomâšek, V., Zlá, S., Fan, Y., 2011. Possible stibnite transformation at the friction surface of the semi-metallic friction composites designed for car brake linings. Appl. Surf. Sci. 258, 1862–1868. https://doi.org/10.1016/j.apsusc.2011.10.063.

Megido, L., Negral, L., Castrillón, L., Marañón, E., Fernández-Nava, Y., Suárez-Peña, B., 2016a. Traffic tracers in a suburban location in northern Spain: relationship between carbonaceous fraction and metals. Environ. Sci. Pollut. Res. 23, 8669–8678. https://doi.org/10.1007/s11356-015-5955-8.

Megido, L., Suárez-Peña, B., Negral, L., Castrillón, L., Suárez, S., Fernández-Nava, Y., Marañón, E., 2016b. Relationship between physico-chemical characteristics and potential toxicity of PM10. Chemosphere 162, 73–79. https://doi.org/10.1016/j.chemosphere.2016.07.067.

Megido, L., Suárez-Peña, B., Negral, L., Castrillón, L., Fernandez-Nava, Y., 2017a. Suburban air quality: human health hazard assessment of potentially toxic elements in PM10. Chemosphere 177, 284–291. https://doi.org/10.1016/j.chemosphere.2017.03.009.

Megido, L., Negral, L., Castrillón, L., Fernandez-Nava, Y., Suárez-Peña, B., Marañón, E., 2017b. Impact of secondary inorganic aerosol and road traffic at a suburban air quality monitoring station. J. Environ. Manag. 189, 36–45. https://doi.org/10.1016/j.jenvman.2016.12.032.

Messori, G., van Wees, D., Pausata, F.S.R., Acosta Navarro, J.C., Hannachi, A., Dentener, F.J., 2018. The impact of future atmospheric circulation changes over the Euro-Atlantic sector on urban PM2.5 concentrations. Tellus Ser. B Chem. Phys. Meteorol. 70, 1–22. https://doi.org/10.1080/16000889.2018.1468704.

Minguillón, M.C., Monfort, E., Escrig, A., Celades, I., Guerra, L., Busani, G., Sterni, A., Querol, X., 2013. Air quality comparison between two European ceramic tile clusters. Atmos. Environ. 74, 311–319. https://doi.org/10.1016/j.atmosenv.2013.04.010.
, .

Moreno, T., Querol, X., Alastuey, A., Reche, C., Cusack, M., Amato, F., Pandolfi, M., Pey, J., Richard, A., Prévt, A.S.H., Furger, M., Gibbons, W., 2011. Variations in time and space of trace metal aerosol concentrations in urban areas and their surroundings. Atmos. Chem. Phys. 11, 9415–9430. https://doi.org/10.5194/acp-11-9415-2011.

Nath, M., Song, S., Li, Y., Xu, Y., 2018. Effect of Cr2O3 addition on corrosion mechanism of refractory castables for waste melting furnaces and concurrent formation of hexavalent chromium. Ceram. Int. 44, 2383–2389. https://doi.org/10.1016/j.ceramint.2017.10.207.

Negral, L., Moreno-Grau, S., Querol, X., Moreno, J., Viana, M., García-Sánchez, A., Alastuey, A., Moreno-Clavel, J., 2012. Weak pressure gradient over the Iberian Peninsula and African dust outbreaks. A new dust long-transport scenario. Bull. Am. Meteorol. Soc. 93, 1125–1132. https://doi.org/10.1175/BAMS-D-10-05000.1.

Pey, J., Alastuey, A., Querol, X., 2013. PM10 and PM2.5 sources at an insular location in the western Mediterranean by using source apportionment techniques. Sci. Total Environ. 456–457, 267–277. https://doi.org/10.1016/j.scitotenv.2013.03.084.
, .

Querol, X., Pérez, N., Reche, C., Ealo, M., Ripoll, A., Tur, J., Pandolfi, M., Pey, J., Salvador, P., Moreno, T., Alastuey, A., 2019. African dust and air quality over Spain: is it only dust that matters?. Sci. Total Environ. 686, 737–752. https://doi.org/10.1016/j.scitotenv.2019.05.349.

Querol, X., Alastuey, A., Lopez-Soler, A., Mantilla, E., Plana, F., 1996. Mineral composition of atmospheric particulates around a large coal-fired power station. Atmos. Environ. 30, 3557–3572. https://doi.org/10.1016/1352-2310(96)00108-2.

Querol, X., Alastuey, A., Viana, M.M., Rodriguez, S., Artiñano, B., Salvador, P., Garcia Do Santos, S., Fernandez Patier, R., Ruiz, C.R., De La Rosa, J., Sanchez De La Campa, A., Menendez, M., Gil, J.I., 2004. Speciation and origin ofPM10 and PM2.5 in Spain. J. Aerosol Sci. 35, 1151–1172. https://doi.org/10.1016/j.jaerosci.2004.04.002.

Querol, X., Viana, M., Alastuey, A., Amato, F., Moreno, T., Castillo, S., Pey, J., de la Rosa, J., Sánchez de la Campa, A., Artíñano, B., Salvador, P., García Dos Santos, S., Fernández-Patier, R., Moreno-Grau, S., Negral, L., Minguillón, M.C., Monfort, E., Gil, J.I., Inza, A., Ortega, L.A., Santamaría, J.M., Zabalza, J., 2007. Source origin of trace elements in PM from regional background, urban and industrial sites of Spain. Atmos. Environ. 41, 7219–7231. https://doi.org/10.1016/j.atmosenv.2007.05.022.

Rudnick, R.L., Gao, S., 2003. Composition of the continental crust. Treatise on Geochemistry 3, 1–64. https://doi.org/10.1016/B0-08-0437516/03016-4.

Saavedra, S., Rodríguez, A., Taboada, J.J., Souto, J.A., Casares, J.J., 2012. Synoptic patterns and air mass transport during ozone episodes in Northwestern Iberia. Sci. Total Environ. 441, 97–110. https://doi.org/10.1016/j.scitotenv.2012.09.014.

Shirmohammadi, F., Wang, D., Hasheminassab, S., Verma, V., Schauer, J.J., Shafer, M.M., Sioutas, C., 2017. Oxidative potential of on-road fine particulate matter (PM2.5) measured on major freeways of Los Angeles, CA, and a 10-year comparison with earlier roadside studies. Atmos. Environ. 148, 102–114. https://doi.org/10.1016/j.atmosenv.2016.10.042.

Sánchez-Rodas, D., Alsioufi, L., Sánchez de la Campa, A.M., González-Castanedo, Y., 2017. Antimony speciation as geochemical tracer for anthropogenic emissions of atmospheric particulate matter. J. Hazard Mater. 324, 213–220. https://doi.org/10.1016/j.jhazmat.2016.10.051.

Shang, J., Wang, K., Zhou, Q., Zhang, D., Huang, J., Li, G., 2012. Microstructure characteristics and mechanical properties of cold metal transfer welding Mg/Al dissimilar metals. Mater. Des. 34, 559–565. https://doi.org/10.1016/j.matdes.2011.05.008.

Stein, A.F., Draxler, R.R., Rolph, G.D., Stunder, B.J.B., Cohen, M.D., Ngan, F., 2015. NOAA's HYSPLIT atmospheric transport and dispersion modeling system. Bull. Am. Meteorol. Soc. 96, 2059–2077. https://doi.org/10.1175/BAMS-D-14-00110.1.

Steinmetz, G.L., Mohan, M.S., Zingaro, R.A., 1988. Characterization of titanium in United States coals. Energy Fuels 2, 684–692. https://doi.org/10.1021/ef00011a015.

Sun, Y., Hu, X., Wu, J., Lian, H., Chen, Y., 2014. Fractionation and health risks of atmospheric particle-bound as and heavy metals in summer and winter. Sci. Total Environ. 493, 487–494. https://doi.org/10.1016/j.scitotenv.2014.06.017.

Sutton, M., Bibby, R.K., Eppich, G.R., Lee, S., Lindvall, R.E., Wilson, K., Esser, B.K., 2012. Evaluation of historical beryllium abundance in soils, airborne particulates and facilities at Lawrence Livermore National Laboratory. Sci. Total Environ. 437, 373–383. https://doi.org/10.1016/j.scitotenv.2012.08.011.

Tsai, J.H., Lin, K.H., Chen, C.Y., Ding, J.Y., Choa, C.G., Chiang, H.L., 2007. Chemical constituents in particulate emissions from an integrated iron and steel facility. J. Hazard Mater. 147, 111–119. https://doi.org/10.1016/j.jhazmat.2006.12.054.

Uria-Tellaetxe, I., Carslaw, D.C., 2014. Conditional bivariate probability function for source identification. Environ. Model. Softw 59, 1–9. https://doi.org/10.1016/j.envsoft.2014.05.002.

US EPA, 2001. Risk Assessment Guidance for Superfund: Volume III — Part A, Process for Conducting Probabilistic Risk Assessment Office of Emergency and Remedial Response. U.S. Environmental Protection Agency, Washington, D.C., USA.

US EPA, 2009. Risk Assessment Guidance for Superfund Volume I: Human Health Evaluation Manual (Part F, Supplemental Guidance for Inhalation Risk Assessment) (Final). EPA-540-R-070e002. OSWER 9285.7-82. Office of Superfund Remediation and Technology Innovation, U.S. Environmental Protection Agency, Washington, D.C., USA.

US EPA, 2014. Risk Assessment for Carcinogenic Effects. U.S. Environmental Protection Agency https://www.epa.gov/fera/risk-assessment-carcinogenic-effects https://www.epa.gov/sites/production/files/2014-05/documents/table1.pdf.

US EPA, 2017. Regional Screening Levels (RSLs) - Generic Tables (May 2017). U.S. Environmental Protection Agency https://www.epa.gov/risk/regional-screening-levels-rsls-generic-tables-november-2017.

Viana, M., Hammingh, P., Colette, A., Querol, X., Degraeuwe, B., Vlieger, I.D., van Aardenne, J., 2014. Impact of maritime transport emissions on coastal air quality in Europe. Atmos. Environ. 90, 96–105. https://doi.org/10.1016/j.atmosenv.2014.03.046.

Vikulin, V.V., Kelina, I.Yu, Shatalin, A.S., Rusanova, L.N., 2004. Advanced ceramic structural materials. Refract. Ind. Ceram. 45, 383–386. https://doi.org/10.1007/s11148-005-0017-2.

Westfall, L.A., Davourie, J., Ali, M., McGough, D., 2016. Cradle-to-gate life cycle assessment of global manganese alloy production. Int. J. Life Cycle Assess. 21, 1573–1579. https://doi.org/10.1007/s11367-015-0995-3.

WHO, 2005. WHO Air Quality Guidelines for Particulate Matter, Ozone, Nitrogen Dioxide and Sulfur Dioxide. WHO Press, World Health Organization, Geneva, Switzerland.

Wu, X., Cobbina, S.J., Mao, G., Xu, H., Zhang, Z., Yang, L., 2016. A review of toxicity and mechanisms of individual and mixtures of heavy metals in the environment. Environ. Sci. Pollut. Res. Int. 23, 8244–8259. https://doi.org/10.1007/s11356-016-6333-x.

Zapico López, E., 2015. Evolution of air quality in the city of Langreo and its relation with emission sources. Doctoral thesis, University of Oviedo, Oviedo